Fast Internal Main-Chain Dynamics of Human Ubiquitin†

Diane M. Schneider,‡,§,∥ Martin J. Dellwo,‡,§,⊥ and A. Joshua Wand*,‡,§,⊥

Department of Biochemistry, University of Illinois at Urbana-Champaign, Urbana, Illinois 61801, and Institute for Cancer Research, Fox Chase Cancer Center, 7701 Burholme Avenue, Philadelphia, Pennsylvania 19111

Received December 16, 1991; Revised Manuscript Received January 31, 1992

ABSTRACT: The fast internal dynamics of human ubiquitin have been studied by the analysis of ^{15}N relaxation of backbone amide nitrogens. The amide ^{15}N resonances have been assigned by use of heteronuclear multiple-quantum spectroscopy. Spin lattice relaxation times at 60.8 and 30.4 MHz and the steady-state nuclear Overhauser effect at 60.8 MHz have been determined for 67 amide ^{15}N sites in the protein using two-dimensional spectroscopy. These data have been analyzed in terms of the model free treatment of Lipari and Szabo [Lipari, G., & Szabo, A. (1982) *J. Am. Chem. Soc. 104*, 4546–4559]. The global motion of the protein is shown to be isotropic and is characterized by a correlation time of 4.1 ns rad^{-1}. The generalized order parameters (S^2) of backbone amide N–H vectors in the globular region of the protein range from 0.5 to 0.95. No apparent correlation between secondary structure and generalized order parameters is observed. There is, however, a strong correlation between the magnitude of the generalized order parameters of a given N–H vector and the presence of hydrogen bonding of the amide hydrogen or its peptide bond associated carbonyl. Using a chemical shift tensor breadth of 160 ppm, the N–H vectors of peptide linkages participating in one or more hydrogen bonds to the main chain show an average generalized order parameter of 0.80 (SD 0.06), while those amide NH of peptide linkages free of hydrogen-bonding interactions with the main chain show an average order parameter of 0.69 (SD 0.06). The last four residues of the C-terminus display a pattern of S^2 values ranging from 0.13 to 0.63 consistent with restricted diffusion about ϕ and ψ rotation axes which is abruptly terminated at residue 72. These data suggest that molecular packing interactions provide the dominant restriction to internal motion on the subnanosecond time scale and that hydrogen-bonding interactions provide a significant but more modest damping of main-chain high-frequency dynamics.

The influence of internal dynamics on protein stability and function continues to be the subject of extensive debate and study [see Careri et al. (1975), Karplus and McCammon (1981), Debrunner and Fraunfelder (1982), Englander and Kallenbach (1984), and Williams (1989) for reviews]. Accordingly, a wide variety of experimental techniques have been employed to characterize the internal motions of biopolymers over a large range of time scales. The use of nuclear magnetic resonance (NMR)[1] spectroscopy, although an inherently rich source of dynamic information in the subnanosecond time scale, has historically been hindered principally by the difficulty in obtaining extensive resonance assignments and primary relaxation data and by the complicated origin of NMR relaxation phenomena. The problems associated with obtaining heteronuclear resonance assignment and primary relaxation data have now been overcome by the development of multidimensional heteronuclear NMR techniques [e.g., Mueller (1979), Bax et al. (1983), Skelnar et al. (1987), Gronenborn et al. (1989), Nirmala and Wagner (1988, 1989), and Kay et al. (1989a,b, 1990, 1991)]. In concert with isotopic enrichment, comprehensive NMR relaxation data have been obtained on a small number of proteins of significant size (Kay et al., 1989a; Clore et al., 1990a).

The extraction of meaningful and unbiased parameters describing relaxation processes has been somewhat simplified by the development of a model-independent formulation by Lipari and Szabo (1982a,b). Here we use this model-free approach to characterize the fast internal dynamics of human ubiquitin. Ubiquitin is a small (76-residue) protein essential to the eukaryotic ATP-dependent protein degradation pathway (Hershko, 1988). For such a small protein, ubiquitin displays a surprising range of secondary structure which includes a five-stranded mixed β-sheet, α-, and 3_{10}-helices and a number of tight turns (Vijay-Kumar et al., 1987; Di Stefano & Wand, 1987). As such, it is ideal as a model system for studies of various aspects of protein structure, stability, and dynamics. This report is focused on the investigation of the range and character of subnanosecond dynamics of the main chain in the native state of the protein. It is directly shown that the overall molecular reorientation of the protein is isotropic and characterized by a correlation time of 4.1 ns rad^{-1}. Generalized order parameters (S^2) and effective correlation times for 67 amide N–H vectors have been obtained. Within the globular

† This work was supported by NIH Research Grants GM-35940 and DK-39806 (A.J.W.), by NIH Grants CA-06927 and RR-05539, by an appropriation from the Commonwealth of Pennsylvania, and by a grant from the F. Ripple Foundation awarded to the Institute for Cancer Research. D.M.S. is the recipient of an NIH postdoctoral fellowship (GM-12594). M.J.D. is the recipient of an NIH predoctoral fellowship administered by the University of Pennsylvania (GM-07229).

* Address correspondence to this author at the University of Illinois.

‡ Fox Chase Cancer Center.

§ University of Illinois at Urbana-Champaign.

∥ Present address: Sterling-Winthrop Research Group, Malvern, PA 19355.

⊥ Present address: Department of Biochemistry, University of Illinois at Urbana-Champaign, Urbana, IL 61801.

[1] Abbreviations: COSY, *J*-correlated spectroscopy; CSA, chemical shift anisotropy; DQF, double-quantum filter; HMQC, heteronuclear multiple-quantum correlation; NOE, nuclear Overhauser effect; NMR, nuclear magnetic resonance; NOESY, NOE-correlated spectroscopy; S^2, generalized order parameter; T_1, spin lattice relaxation time; τ_e, effective correlation time; τ_m, global isotropic correlation time; TOCSY, total correlation spectroscopy.

0006-2960/92/0431-3645$03.00/0

portion of the protein, the S^2 values range from 0.5 to 0.95. There is no apparent correlation between the magnitude of the S^2 of given N–H vector and the type of secondary structure in which it is located. There is, however, strong indication of a more general correlation between S^2 and the participation of the associated peptide linkage in one or more hydrogen bonds to the main chain. These and other observations lead to the conclusion that molecular packing interactions provide the dominant restriction to high frequency motion of the main chain with hydrogen-bonding interactions providing a significant but more modest reduction.

Materials and Methods

Sample Preparation. Ubiquitin was uniformly labeled with ^{15}N by growth of *Escherichia coli* harboring the expression vector pNMHUB (Ecker et al., 1987) on ^{15}N-labeled Celtone (Martek). Ubiquitin was purified as described (Ecker et al., 1987) except that gel filtration on Sephadex G-50 (Pharmacia) was substituted for ion exchange chromatography. All solvents and buffers were reagent grade and were used without further purification. Protein purity was assessed by electrophoresis on 18% polyacrylamide gel.

Samples were 2 mM in ubiquitin, with 50 mM potassium phosphate (90% H_2O/10% D_2O), adjusted to pH 5.0 or 5.8 (uncorrected for the isotope effect) as required. For the relaxation studies, the sample was deoxygenated with argon and sealed in a 5-mm NMR tube. Proton chemical shifts are referenced to an external standard of sodium 3-(trimethylsilyl)tetradeuteriopropionate in D_2O. Nitrogen chemical shifts are referenced to external $(^{15}NH_4)_2SO_4$ at 24.93 ppm.

NMR Spectroscopy. Analysis of DQF COSY (Rance et al., 1983), HMQC (Mueller, 1979; Bax et al., 1983), HMQC-TOCSY and HMQC-NOESY (Gronenborn et al., 1989) spectra provided ^{15}N assignments for the amide nitrogen resonances in ubiquitin. These experiments were performed at 30 °C on a Bruker AM-600 spectrometer. All experiments were performed during the same experimental session in order to facilitate comparison of chemical shift information. All were obtained with time-proportional phase incrementation (TPPI) to provide quadrature detection during the incremented time domain (Marion & Wüthrich, 1983) and ^{15}N WALTZ-16 decoupling during acquisition (Shaka et al., 1983). A WALTZ pulse train was used to promote mixing in the HMQC-TOCSY experiment. Mixing times for the TOCSY and the NOESY were 30 and 100 ms, respectively. The sweep width was 7042 Hz in the proton dimension and 4000 Hz in the nitrogen dimension. A total of 1024 complex points were collected for each free induction decay. All spectra were the result of signal averaging at least 32 scans per FID with four dummy scans. A total of 650 FIDs were collected for the COSY and the HMQC experiments. 700 and 750 FIDs were collected for the HMQC-TOCSY and HMQC-NOESY, respectively. Solvent suppression was done by the method of direct presaturation with low-power irradiation during the recycle delay of 1.5 s.

^{15}N T_1 relaxation times and ^{15}N NOEs of the amide resonances in ubiquitin were measured at 60.8 (Bruker AM-600 spectrometer) and 30.4 MHz (Bruker AM-300 spectrometer). Longitudinal relaxation of amide ^{15}N nuclei was measured using the two-dimensional sampling technique of Nirmala and Wagner (1988). The T_1 recovery period in the relaxation experiment was varied so that the time course would span at least two T_1s. Broadband proton saturation was applied during this delay to ensure that the inversion–recovery curve is a single exponential in order to avoid potential systematic bias arising from coupling of ^{15}N populations to evolving ^1H magnetization (Dellwo & Wand, 1991) and interference effects arising from cross correlation with CSA (see below). Proton saturation was achieved by application of multiples of four evenly spaced (15-ms) 90° pulses. The proton and nitrogen sweep widths at 60.8 MHz are as described above. The spectra at 30.4 MHz were collected with a sweep width of 2000 Hz in the proton dimension and 2000 Hz in the nitrogen dimension. Each spectrum was the result of signal averaging 64 scans per FID with four dummy scans. A total of 1024 complex points were collected in t_2 and 320 FIDs were collected in t_1. The spectra were processed to 2048 by 2048 real points. The T_1 relaxation curve was sampled at eight time points for data acquired at 30.4 MHz (65, 125, 185, 245, 305, 365, 485, and 605 ms) and at ten time points for data acquired at 60.8 MHz (65, 125, 185, 245, 305, 365, 485, 605, 905, and 1205 ms). Solvent suppression and quadrature detection in the incremented time domain were achieved as above. Cross-peak volumes were corrected for baseline offset by local integration around each cross-peak. These corrections were generally small, on the order of 3%. The T_1 relaxation time constant for each amide nitrogen resonance was extracted from a least-squares regression of the logarithm of cross-peak volume as a function of relaxation delay.

Nuclear Overhauser effects were determined from a data set consisting of two heteronuclear 2D spectra measured according to the scheme of Kay et al. (1990) at 60.8 MHz. To develop the NOE, protons were saturated for 3 s. Control experiments indicate that zero proton magnetization was obtained within 100 ms. Control experiments also confirmed that the 3-s proton saturation period was sufficient to reach the steady-state NOE. Each spectrum was the result of signal averaging 256 scans per FID with four dummy scans. Quadrature detection in the incremented time domain was achieved by time-proportional phase incrementation. The value of the NOE was obtained from the ratio of the peak volume obtained with proton saturation to the peak volume obtained without proton saturation. Volumes were corrected for baseline offsets as described above.

All spectra were processed with FTNMR and FELIX software (Hare Research, Inc., Bothell, WA). Numerical analysis of relaxation data was done on a Silicon Graphics Personal Iris 4D/25 using software described previously (Dellwo & Wand, 1989).

Theory

The ^{15}N relaxation data have been analyzed according to the model-free approach developed by Lipari and Szabo (1982a,b). This approach allows relaxation phenomena to be interpreted using the minimum number of parameters required to express the unique information about the motions underlying the relaxation process without the need to make specific assumptions about their exact physical character. The dipolar contribution to the spin lattice relaxation time (T_1^{dd}) is given by (Wittebort & Szabo, 1978)

$$\frac{1}{T_1^{dd}} = \frac{\hbar^2\gamma_H^2\gamma_N^2}{4r_{NH}^6}[J(\omega_H - \omega_N) + 3J(\omega_N) + 6J(\omega_H + \omega_N)] \quad (1)$$

where r_{NH} is taken to be 1.02 Å, ω is the Larmor frequency in rad s^{-1}, $\hbar$ is given in units of erg s rad^{-1} (equivalent to G^2 cm^3 s rad^{-1}), and γ is in units of rad s^{-1} G^{-1}. Both T_1 and associated correlation times (see below) are in s rad^{-1}. The above expression for T_1 corresponds to dipolar mediated ^{15}N relaxation in the presence of continuous decoupling of protons. To include the contribution of chemical shift anisotropy (CSA)

to the observed spin lattice relaxation time, eq 1 is combined with

$$\frac{1}{T_1^{csa}} = \frac{1}{3}\Delta\delta^2\omega_N^2 J(\omega_N) \quad (2)$$

where the breadth of the chemical shift tensor, $\Delta\delta$, is given in parts per million (ppm). Thus the expression used in the analysis of T_1 relaxation is given by

$$\frac{1}{T_1} = \frac{1}{T_1^{dd}} + \frac{1}{T_1^{csa}} \quad (3)$$

The NOE is then given by

$$\text{NOE} = 1 + \frac{\gamma_H}{\gamma_N}\left(\frac{\hbar\gamma_H^2\gamma_N^2}{4r_{NH}^6}\right)[6J(\omega_H + \omega_N) - J(\omega_H - \omega_N)]T_1 \quad (4)$$

Within the framework of the model free treatment, a simple form for the spectra density function $J(\omega)$ is proposed. For a N–H vector attached to an isotropically reorienting molecule, the spectral density is given by (Lipari & Szabo, 1982a)

$$J(\omega) = \frac{2}{5}\left[\frac{S^2\tau_m}{(1 + \omega^2\tau_m^2)} + \frac{(1 - S^2)\tau}{(1 + \omega^2\tau^2)}\right] \quad (5)$$

where

$$1/\tau = 1/\tau_m + 1/\tau_e$$

Here, τ_m is the correlation time describing the overall isotropic motion of the molecule, S^2 is the generalized order parameter and corresponds to the limiting value for the decay of the autocorrelation function due to internal motion, and τ_e is an effective correlation time for the reorientation of the N–H vector due to internal motion and is formally defined as the area of the internal correlation function. In cases where the overal motion cannot be described by a single correlation time (i.e., it is anisotropic), an approximation can be made to express the spectral density as (Lipari & Szabo, 1982a)

$$J(\omega) = \frac{2}{5}\left\{S^2\left[\frac{A\tau_1}{(1 + \omega^2\tau_1^2)} + \frac{(1 - A)\tau_2}{(1 + \omega^2\tau_2^2)}\right] + (1 - S^2)\left[\frac{A\tau_{1e}}{(1 + \omega^2\tau_{1e}^2)} + \frac{(1 - A)\tau_{2e}}{(1 + \omega^2\tau_{2e}^2)}\right]\right\} \quad (6)$$

where

$$1/\tau_{1e} = 1/\tau_1 + 1/\tau_e$$

and

$$1/\tau_{2e} = 1/\tau_2 + 1/\tau_e$$

The two correlation times τ_1 and τ_2 and the mixing parameter A describe global anisotropic motion. A is a mixing coefficient that can, in principle, adopt a value between 0 and 1. In the limit of isotropic motion, $\tau_1 = \tau_2$ and A is meaningless.

Results

Assignment of ^{15}N Amide Resonances. The ^1H spectrum of human ubiquitin has been assigned by us and others (Di Stefano & Wand, 1987; Weber et al., 1987). These resonance assignments served as a starting point for the assignment of backbone amide nitrogen resonances of the protein. Comparison of ^{15}N–^1H chemical shift correlations provided by the HMQC spectrum with the amide–α ^1H–^1H chemical shift correlations of the DQF-COSY spectrum (Di Stefano & Wand, 1987) provided a set of possible identities for each ^{15}N resonance. For approximately one-third of the ^{15}N–^1H cross-peaks in the HMQC spectrum, the chemical shift of the amide ^1H resonance was nondegenerate and therefore directly provided an uniequivocal identification of the associated amide ^{15}N resonance. In most cases, however, there were two or more candidates for the identity of the amide ^1H resonance of a given ^{15}N–^1H correlation in the HMQC spectrum. These ambiguities were resolved by using the HMQC-TOCSY spectrum to provide longer range correlations of a given ^{15}N–^1H cross-peak with ^1H resonances of the attached side-chain spin system (not shown). In most cases the provision of the chemical shift of the α ^1H resonance was sufficient to provide unequivocal identification of the ^{15}N–^1H cross-peak. For example, the amide hydrogen resonances of V26, K29, and N60 have nearly degenerate amide ^1H resonances, which results in ambiguity in the assignment of the associated ^{15}N resonances by reference to the HMQC spectrum alone. This ambiguity is removed by the HMQC-TOCSY experiment which provides long-range correlations between the ^{15}N resonance and the α and other hydrogen resonances of the same residue. A unique identity could thereby be established for each amide nitrogen frequency. As a final test of the correctness of the ^{15}N resonance assignments obtained by this approach, the HMQC-NOESY spectrum was used to confirm that previously documented main-chain ^1H–^1H NOEs (Di Stephano & Wand, 1987) were indeed correlated with the appropriate ^{15}N resonances. An example is shown in Figure 1 where the anticipated amide ^1H–^1H NOEs occurring within the α-helical segment spanning residues 30–36 are correlated with the appropriate ^{15}N resonances. The resulting assignments for the backbone amide ^{15}N resonances of human ubiquitin are listed in Table I.

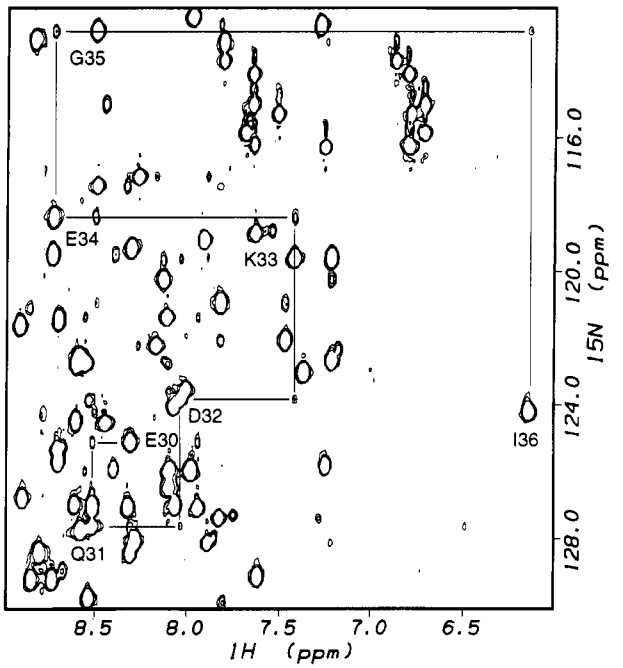

FIGURE 1: Expansion of a NOESY-HMQC spectrum of human ubiquitin used to provide final confirmation of ^{15}N resonance assignments by the correlation of ^1H–^1H NOEs with the appropriate ^{15}N resonance. Shown are the ^1H–^1H NOEs between amide NH of the α-helix of ubiquitin. An NOE mixing time of 100 ms was used.

Measurement of Relaxation Parameters. T_1 and NOE relaxation parameters for 67 of 73 possible backbone amide ^{15}N sites could be unambiguously extracted from inversion–recovery profiles obtained at 14.1 T. A small number of ^{15}N–^1H cross-peaks were ill-resolved at 30.2, MHz and the derived model-free parameters for these sites were based solely

Table I: ^{15}N Resonance Assignments and Obtained Model-Free Parameters for Human Ubiquitin[a,b]

residue	^{15}N (ppm)	S^2	τ_e (ps rad^{-1})	residue	^{15}N (ppm)	S^2	τ_e (ps rad^{-1})
Gln 2	126.9	0.89	12	Arg 42	127.0	0.76	~0
Ile 3	119.3	0.84	~0	Leu 43	128.3	0.92	~0
Phe 4	122.4	nd[c]	nd	Ile 44	126.0	0.69	~0
Val 5	125.1	0.75	~0	Phe 45	129.4	0.75	~0
Lys 6[d]	131.7	0.84	10	Ala 46	136.8	0.83	~0
Thr 7	119.5	0.85	~0	Gly 47	106.5	0.83	~0
Leu 8	125.3	0.72	~0	Lys 48	125.9	0.69	1
Thr 9	109.8	0.70	~0	Gln 49[d]	126.7	0.69	5
Gly 10	113.1	0.67	2	Leu 50	129.8	0.74	~0
Lys 11	112.5	0.79	~0	Glu 51	127.0	0.73	~0
Thr 12	124.5	0.74	~0	Asp 52[d]	123.9	0.67	~0
Ile 13	131.6	0.81	~0	Gly 53[e]	111.6	nd	nd
Thr 14	125.8	0.76	~0	Arg 54	123.0	0.78	~0
Leu 15	129.1	0.80	~0	Thr 55	112.9	0.64	~0
Glu 16[d]	126.4	0.73	~0	Leu 56	122.1	0.87	~0
Val 17	121.5	0.76	~0	Ser 57	117.1	0.82	~0
Glu 18	122.7	nd	nd	Asp 58	128.0	0.86	~0
Ser 20	125.8	0.61	15	Tyr 59	119.6	0.74	~0
Asp 21	127.3	0.71	~0	Asn 60	120.2	0.72	~0
Thr 22	112.2	0.79	~0	Ile 61	122.6	0.77	~0
Ile 23[d]	125.1	0.82	~0	Gln 62	129.1	0.86	59
Asn 25[d]	123.5	0.77	~0	Lys 63	124.5	0.69	~0
Val 26[d]	125.9	0.77	11	Gly 64	118.3	0.81	44
Lys 27[d]	122.6	nd	nd	Ser 65	118.9	0.83	~0
Ala 28	127.0	0.76	~0	Thr 66	121.3	0.82	~0
Lys 29	121.4	0.79	~0	Leu 67[d]	131.5	0.75	~0
Ile 30	125.1	0.74	~0	His 68	123.6	0.77	~0
Gln 31	127.6	0.79	~0	Leu 69	128.3	0.76	~0
Asp 32[d]	123.8	0.72	4	Val 70	130.8	0.84	~0
Lys 33	119.6	0.75	~0	Leu 71	127.0	0.74	~0
Glu 34	118.2	0.76	~0	Arg 72	127.7	0.79	~0
Gly 35	112.8	0.75	~0	Leu 73	128.5	0.63	57
Ile 36	124.2	0.69	~0	Arg 74	125.9	0.47	83
Asp 39	117.4	0.85	~0	Gly 75	115.0	0.27	147
Leu 40	120.9	0.69	~0	Gly 76	118.9	0.13	100
Gln 41[d]	121.1	0.77	~0				

[a] Resonance assignments for 2 mM ubiquitin in 50 mM potassium phosphate buffer, pH 5.0, at 20 °C. ^{15}N chemical shifts are referenced to external $(^{15}NH_4)_2SO_4$ at 24.93 ppm. [b] Relaxation data obtained at 20 °C, pH 5.0, 50 mM potassium phosphate buffer. For each ^{15}N site, model-free parameters have been calculated using a value of 160 ppm for the breadth of the chemical shift tensor ($\Delta\sigma$), 1.02 Å for the N–H bond length and 4.125 ns rad^{-1} for the isotropic correlation time for molecular reorientation. [c] nd, not determined due to insufficient resolution for all data. [d] Model-free parameters determined using 60.8-MHz data only due to lack of resolution and/or poor regression statistics for data collected at 30.4 MHz. [e] Not observed at 20 °C and pH 5.0, the given chemical shift is for 30 °C and pH 5.8.

on data obtained at 60.4 MHz (see Table I). Shown in Figure 2 are plots of longitudinal relaxation curves which correspond to T_1 relaxation rates that span the range of T_1 values observed. In general, excellent linear correlation of the semilogarithmic plots was seen for data at both fields, indicating that the relaxation is governed by a single exponential which is critical to the accuracy of subsequent analysis (Dellwo & Wand, 1991). With the exception of the four carboxy-terminal residues, the values of the T_1 relaxation time constants are fairly uniform throughout the main body of the protein. The last four residues of the protein, which are known to be unstructured in solution (Di Stephano & Wand, 1987), have significantly longer amide nitrogen longitudinal relaxation time constants.

Figure 3 shows expansions of the ^{15}N–^1H chemical shift correlation spectra acquired without (top panel) and with the NOE (bottom panel). As the ^{15}N nucleus has a negative gyromagnetic ratio the volume of the cross-peaks is expected to decrease under the action of the NOE.

Characterization of Global Motion. A critical feature of the model-free approach of Lipari and Szabo (1982a) is the requirement that the total correlation function governing relaxation be successfully factored into a product of correlation functions corresponding to global and internal motion. This is only rigorously possible when the global motion corresponding to molecular tumbling is isotropic and the time scale for this motion is much slower than that describing the internal

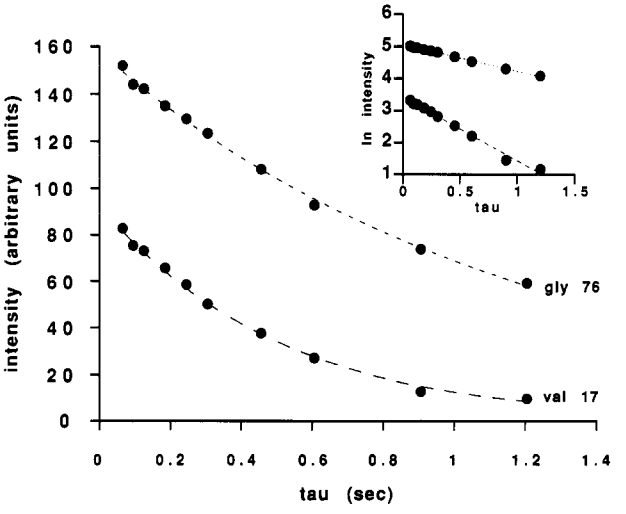

FIGURE 2: T_1 relaxation curves obtained at 60.4 MHz for Gly 76 (top) and Val 17 (bottom). These curves are defined by spin lattice relaxation times which span the range observed in human ubiquitin. The inset shows the corresponding semilogarithmic plots.

motion. This premise can be explicitly examined in cases where the experimental relaxation data set results in the overdetermination of the global and internal model-free parameters (Dellwo & Wand, 1989). Using the general form of the model-free spectral density function, which allows for aniso-

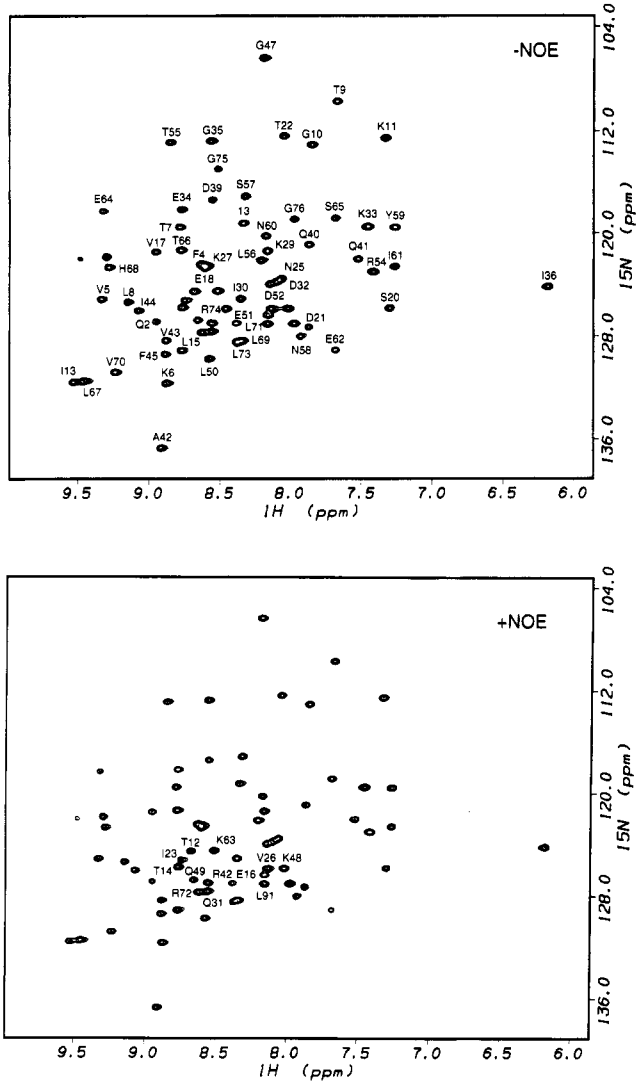

FIGURE 3: ^1H–^{15}N chemical shift correlation spectra of human ubiquitin obtained without (top panel) and with (bottom panel) the NOE. Both spectra a plotted with the same scaling. Sequence-specific resonance assignments are indicated.

tropic global motion, the relaxation data from M nuclei can be described by three global parameters (τ_1, τ_2, A) and M sets of model-free parameters (S^2, τ_e). Using the $3M$ observables (T_1 at two fields, NOE at one field), the character of the global motion can be determined by finding the values of τ_1, τ_2, and A which best reproduce the primary relaxation data. The target function whose minimum is sought is defined as the sum of the squares of the fractional differences between calculated and observed values of the primary T_1 and NOE data (Dellwo & Wand, 1989), i.e.,

$$\text{Error} = \sum_{\omega}\sum_{j}^{M}\left(\frac{T_1^{obs} - T_1^{calc}}{T_1^{obs}}\right)_j + \left[\frac{(NOE/T_1)^{obs} - (NOE/T_1)^{calc}}{(NOE/T_1)^{obs}}\right]_j \quad (7)$$

where the sums are over all fields used and the M sites for which data is available. As before, the NOE is divided by T_1 to avoid double counting the contribution of T_1 to the error function (see eq 4). The gradients of this target function are generally shallow, and the minimum is most efficiently found by an explicit search of all reasonable ranges of τ_1, τ_2, and A (Dellwo & Wand, 1989). In the present case, the grid search spanned values of τ_1 and τ_2 of 2–8.0 ns in 0.125-ns steps and of A ranging from 0 to 1 in 0.05 steps. At each set of

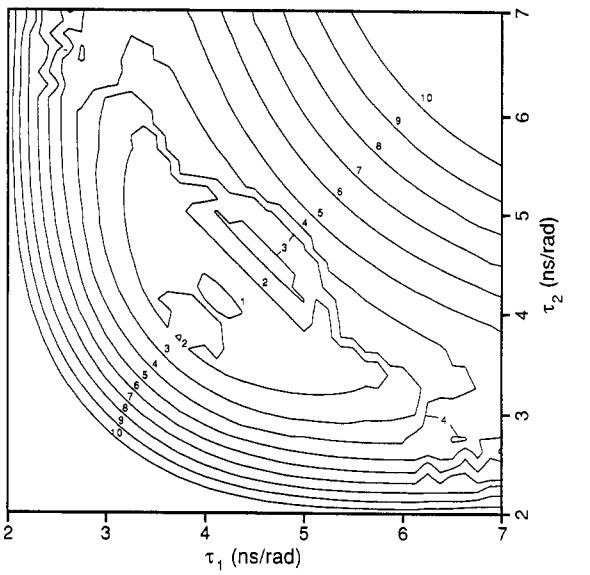

FIGURE 4: Contour plot of the error defined by eq 7 as a function of τ_1 and τ_2 for $A = 0.5$. The minimum occurs at $\tau_1 = \tau_2 = 4.125$ ns rad^{-1}. This demonstrates that human ubiquitin tumbles isotropically. The contours drawn span a factor of 2 in the magnitude of the error.

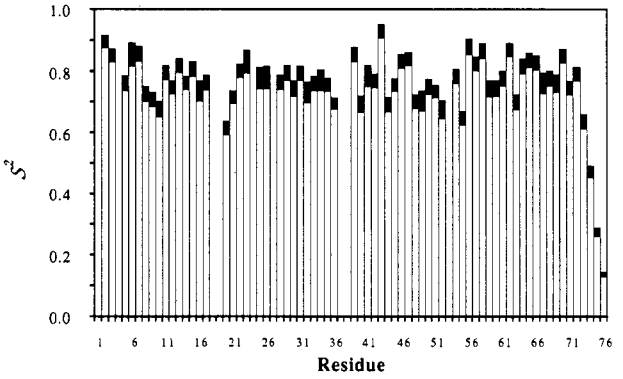

FIGURE 5: Generalized order parameters of N–H vectors of human ubiquitin. The lower and upper values of the generalized order parameter were obtained using 170 and 140 ppm for $\Delta\delta$ (see eq 2). The calculations assumed an effective N–H bond length of 1.02 Å and used the determined isotropic correlation time of 4.125 ns rad^{-1} (see the text and Figure 4).

values of global parameters, the best model-free parameters for each set were determined. The calculated observables were then used to generate the error function defined by eq 7. The resulting error function is a three-dimensional grid. The three-dimensional error grid can be displayed as separate planes showing contours of errors versus τ_1 and τ_2. One such plane is shown in Figure 4 for $A = 0.5$. The global minimum of the target function was found at $\tau_1 = \tau_2 = 4.125$ ns. No unique minimum was found in the global A parameter. Indeed a trough of minima is observed along the A coordinate. These findings demonstrate that the global motion of ubiquitin in solution is, as might be expected, isotropic and defined by a single global correlation time of 4.1 ± 0.1 ns.

Characterization of Internal Motion. The explicit demonstration that ubiquitin is undergoing isotropic global motion allows the fully rigorous isotropic form of the model-free theory to be applied to the description of the internal motion of the backbone amide N–H vectors. Using the correlation time for molecular reorientation determined above, the generalized order parameter and effective correlation time describing the motion of each N–H vector were determined by nonlinear regression. These calculations assumed a constant N–H bond length of 1.02 Å and were done using chemical shift tensor

breadths of 140, 160, or 170 ppm. The S^2 and τ_e values obtained using a $\Delta\delta$ of 160 ppm are listed in Table I, and the range of S^2 values obtained by using 140 and 170 ppm for $\Delta\delta$ is shown in Figure 5. With the exception of residues 74, 75, and 76, the generalized order parameters of the backbone N–H vectors fall between 0.5 and 0.95 with the majority being centered around a value of 0.8. The effective correlation times obtained for *all* backbone N–H vectors are less than 150 ps. This is an especially important result as it indicates that, for all amide N–H vectors examined, $\tau_e \ll \tau_m$. This satisfies a fundamental premise of the most rigorous form of the model-free treatment. Generally satisfactory regressions were obtained although a few fits gave residuals in excess of 10%. These could, however, be explained by poor fits of the primary relaxation data. Overall, the regression statistics of the model-free fits indicate that the internal motion leading to relaxation can, at every site, be adequately described by a single set of model-free parameters. The data obtained on the native state of human ubiquitin provide no indication of a separation of time scales of two or more classes of internal motion. Such a case would require analysis with a form of the model-free theory in which the correlation function describing internal motion is further factored into two or more correlation functions (Clore et al., 1990b). An example of this behavior was observed for several sites in interleukin 1β (Clore et al., 1990a).

Discussion

Reliability of Primary Relaxation Data. The primary relaxation data obtained by the use of two-dimensional heteronuclear J-correlated spectroscopy are of generally high precision. However, as will become clear below, the dominant sources of potential inaccuracy of the obtained model-free parameters find their origin in the various assumptions used in the analysis of the NOE and T_1 relaxation parameters extracted from the primary relaxation data.

The analysis of longitudinal relaxation profiles used here, as with most studies of this kind, assumes that the recovery to equilibrium is governed by a single exponential. The relaxation behavior of freely evolving dipolar coupled spin systems is multiexponential (Solomon, 1955). It has recently been shown that model-free generalized order parameters obtained from T_1 relaxation curves of fully coupled systems are exposed to upward bias with the effect being most pronounced on small S^2 values (Dellwo & Wand, 1991). However, these issues are avoided by use of the pulse sequence of Nirmala and Wagner (1988) which incorporates broadband ^{1}H decoupling during the ^{15}N relaxation period. This not only ensures that dipolar mediated relaxation is uniformly monoexponential but also eliminates concern regarding potential effects arising from chemical exchange of backbone amide hydrogens with solvent. It should also be pointed out that, under the conditions used here (pH 5.0, 20 °C), the predicted (Molday et al., 1972) intrinsic exchange rates are generally an order of magnitude too slow for chemical exchange with solvent to contribute to the apparent rate of longitudinal relaxation. In summary, these effects can be confidently considered to be negligible and not to contribute significantly to multiexponential behavior.

A potentially more serious source of inaccuracy in the obtained model-free parameters is the influence of chemical shift anisotropy (CSA) on the relaxation of ^{15}N nuclei by bonded hydrogen. The presence of significant chemical shift anisotropy leads to coupled equations describing the evolution of longitudinal magnetization of both ^{15}N and its bonded ^{1}H [Goldman (1984); see also Boyd et al. (1990)]:

$$d\langle S_z\rangle/dt = -A_1[S_z - 2S_0] - B_1\langle 2S_zI_z\rangle - E_1[I_z - 2I_0] \quad (8a)$$

$$d\langle I_z\rangle/dt = -A_1[I_z - 2I_0] - E_1[S_z - 2S_0] \quad (8b)$$

$$d\langle 2S_zI_z\rangle/dt = -C_1\langle 2S_zI_z\rangle - B_1[S_z - 2S_0] \quad (8c)$$

where spins S and I correspond here to ^{15}N and ^{1}H, respectively. The coefficients are constants where A_1 is the total T_1 defined by eq 3. This system of coupled equations predicts multiexponential behavior of spin lattice relaxation in fully coupled systems and would result in systematic bias of obtained model-free parameters in a manner analagous to that described elsewhere (Dellwo & Wand, 1991). However, in addition to removing time-dependent dipolar-mediated coupling of ^{15}N to ^{1}H spins (see above), the saturation of protons during the ^{15}N relaxation period also leads to the suppression of the I_zS_z coherence. This effectively decouples CSA from dipolar relaxation processes. Thus one would predict that the presence of significant CSA would not, under the pulse sequence used here, result in multiexponential behavior of obtained T_1 relaxation profiles. Indeed, as indicated by Figure 2, the inversion–recovery profiles, over the range of dynamics present in ubiquitin, are decidedly single exponential in character.

Reliability of Obtained Model-Free Parameters. Given that the primary relaxation data are limited only by their inherent precision and are not corrupted by multiexponential behavior, there remain two significant concerns regarding the influence of chemical shift anisotropy on the interpretation of relaxation by use of the model-free treatment. One is the potential uncertainty of the magnitude of the constant contribution of CSA to the observed rate of longitudinal recovery to equilibrium (see eqs 1 and 8a). The constant contribution of CSA to T_1 can be large and is field dependent. For example, for an internally rigid N–H vector tumbling with an isotropic correlation time of 4.1 ns rad^{-1}, an ^{15}N CSA of 160 ppm results in a contribution to the observed T_1 of approximately 5% and 20% at 30.2 and 60.4 MHz, respectively. There is, unfortunately, a paucity of data regarding the sequence dependence of the size and nature of the chemical shift tensor decribing CSA for amide ^{15}N nuclei. The breadths ($\Delta\delta$) of the chemical shift tensors appear to range from 140 to 170 ppm (Hartzell et al., 1987; Hiyama et al., 1988). It should also be noted that motional averaging of the N–H bond can lead to potential scaling effects on S^2 [see Henry and Szabo (1985)]. However, studies of model compounds indicate little variance (<0.02 Å) in the equilibrium N–H bond length (Taylor & Kennard, 1983).

Most generalized order parameters determined are large (>0.60) and have associated effective correlation times of less than 50 ps. As pointed out previously (Lipari & Szabo, 1982a; Dellwo & Wand, 1989), under these conditions the obtained generalized order parameters are anticipated to be of high accuracy with associated error linearly dependent upon the accuracy of the relaxation parameters used to obtain them. Accordingly, for the majority of model-free parameters obtained, the associated regression statistics indicate a relative error of less than 5%. In this limit, however, the effective correlation times are less well determined.

Correlation of Fast Internal Motion with Structure. The obtained model-free generalized order parameters of backbone amide N–H vectors in human ubiquitin provide an interesting insight into the relationship between globular protein structure and subnanosecond dynamics. The generalized order parameter is a direct measure of the amplitude of internal motion contributing to relaxation and ranges from 1 (completely rigid) to 0 (Lipari & Szabo, 1982a). Even with the exclusion of the last four residues of the protein, the range of amplitudes of

backbone dynamics of human ubiquitin, as quantitated by the generalized order parameters of amide N–H vectors, is somewhat broader than seen in similar studies of staphylococcal nuclease (Kay et al., 1989a) and interleukin 1β (Clore et al., 1990a). As was observed for these two proteins, we find no apparent correlation between the generalized order parameter and secondary structure in human ubiquitin. However, a more general correlation is observed between the obtained generalized order parameter and the presence of hydrogen bonding of the amide NH and/or its peptide linkage associated carbonyl. For the purpose of discussion, we group the amide NH into two classes. One class is composed of amide NH which are hydrogen bonded to main-chain acceptors or whose rigid body associated (i.e., residue i–1) carbonyl is hydrogen bonded to a main-chain donor. The second class is formed by all amide NH that fail to meet the hydrogen-bonding criteria of the first class. Comparison of the crystal structure of human ubiquitin (Vijay-Kumar et al., 1987) and our preliminary model for the solution structure[2] reveals a general correspondence between the two models. However, several subtle differences have been found which will bear on the following analysis. The crystal structure indicates a unusual β-bulge conformation involving residues 7–12 which includes a hydrogen bond between O7 and NH10. The solution structure indicates the presence of a β-bulge with hydrogen bonding between O7 and NH11. In contrast to the crystal structure, the solution structure of human ubiquitin indicates that NH62 is hydrogen bonded (to O60), NH63, O62, O54, and NH20 are not hydrogen bonded to the main chain, and O53 and NH47 are hydrogen bonded to NH23 and O45, respectively. If one takes the hydrogen bonding of the solution structure and assumes a uniform CSA tensor breadth of 160 ppm, it is found that the amide NH of the first class defined above have an average S^2 of 0.80 (0.06). There are 52 such amide sites. In the diffusion in a cone model (Lipari & Szabo, 1981a,b), this corresponds to motion within a semiangle of 21°. The average S^2 of the second class (excluding residues 73–76) is 0.69 (0.06), which corresponds to a cone semiangle of 28°. There are 11 amide sites in this group. Inclusion of the four C-terminal residues lowers the mean S^2 value of the non-hydrogen-bonded class to 0.60. Application of the null hypothesis indicates that the distinction of the two classes is statistically significant ($p < 0.01$). A correlation between the presence of hydrogen bonding and reduced amplitude of motion of the peptide linkage is therefore indicated. There are, however, apparent exceptions to the correlation. For example, though both the crystal and preliminary model for the solution structure of ubiquitin indicate that HN22 is not hydrogen bonded to the main chain, the generalized order parameter for this N–H vector is large (0.79). Similarly, while the generalized order parameter for NH48 is low (0.69), both the solution and crystal structures indicate the presence of a hydrogen bond to O45.

Although previous studies of this type have usually assumed a uniform CSA tensor breadth of 160 ppm (Kay et al., 1989; Clore et al., 1990), there is evidence for significant variation of $\Delta\delta$ (Hartzell et al., 1987; Hiyama et al., 1988). If one assumes the worst case scenario with respect to the correlation of hydrogen bonding with S^2 (i.e., using $\Delta\delta$ of 140 ppm for hydrogen-bonded sites and $\Delta\delta$ of 170 ppm for non-hydrogen-bonded sites which will lower and raise the obtained S^2 values, respectively), one finds that distinction between the mean S^2 of the hydrogen-bonded class and that of the non-hydrogen-bonded class is still maintained ($p < 0.01$). Finally, it is tempting to ascribe the correlation of S^2 with hydrogen bonding to systematic changes in the effective N–H bond length. However, the fact that hydrogen bonding of *either* the NH or the associated carbonyl is sufficient for the correlation argues against this. Furthermore, if the actual effective N–H bond length is longer in the presence of hydrogen bonding, then the obtained S^2 (using the constant, shorter bond length) will actually be smaller than the true value (i.e., the effect of hydrogen bonding on S^2 is stronger than detected).[3]

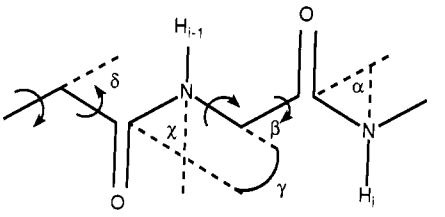

FIGURE 6: Definition of the rotation axes and relevant angles for the analysis of restricted diffusion at the C-terminus of human ubiquitin using eq 11. The angles α, β, γ, δ, and χ correspond to rigid angles of 60°, 70.5°, 0°, 70.5°, and 60°, respectively.

Table II: Model-Free Analysis of Restricted Diffusion at the C-Terminus of Human Ubiquitin[a]

residue	S^2_{obs}	S^2_{rec}
Arg 72	0.79	
Leu 73	0.63	0.80
Arg 74	0.47	0.75
Gly 75	0.27	0.57
Gly 76	0.13	0.48

[a] S^2_{rec} corresponds to the recursive ratio of $S^2_i/S^2_{(i-1)}$ beginning with residue 72.

Main-Chain Dynamics at the C-Terminus. The generalized order parameters of the amide N–H vectors of residues 72–76 are particularly simple to interpret in the context of a specific motional model. The generalized order parameter of a particular amide N–H vector can be expressed as a product of the order parameters of successive rotation axes such that (Lipari & Szabo, 1982b)

$$S^2_{obs}(\text{N–H})_i = \prod_j S^2(\theta_j) \tag{9}$$

where the index i corresponds to the ith residue and the index j corresponds to the jth rotation axis. In the limit of free rotations, $S^2_j = [P_2(\cos\theta_j)]^2$, where θ_j is the angle between the jth and (j–1)th rotational axes (Lipari & Szabo, 1982b; Wallach, 1967). A more complicated form in the case of restricted rotations can be specified where (Lipari & Szabo, 1982b)

$$S^2_j = [P_2(\cos\theta)]^2 + \frac{3\sin^2\theta\sin^2\phi}{\phi^2}\left(\cos^2\theta + \frac{1}{4}\sin^2\theta\cos^2\phi\right) \tag{10}$$

Here the motion about the axis (j–1) is restricted to within some angle ($\pm\phi$) away from the "equilibrium" conformer. In either case, for $\theta_j = 0$ then $S^2_j = 1$. Assuming a rigid planar peptide bond with sp^2 geometry, the angle between successive rotational axes $(\text{N–C}_\alpha)_{i-1}$ and $(\text{C}_\alpha\text{–C}')_{i-2}$ is equal to 0 (see

[2] Our current model for the solution structure of human ubiquitin is based on a family of 32 structures. At the current stage of refinement, these structures give an average rmsd of main-chain N, C′, C$_\alpha$, and O atoms from the mean structure of less than 1.1 Å. The refinement is still in progress.

[3] This is only strictly true when τ_e approaches zero, which is the case for all but a few sites in human ubiquitin.

Figure 6). It is then easily shown that

$$\frac{S^2_{obs}(N\text{-}H)_i}{S^2_{obs}(N\text{-}H)_{i-1}} = \frac{S^2(\alpha)S^2(\beta)S^2(\gamma)S^2(\delta)}{S^2(\chi)S^2(\delta)} = \frac{S^2(\alpha)S^2(\beta)}{S^2(\chi)} \quad (11)$$

which, in the limit of completely free rotation, reduces to 0.111. Using residue 72 as a starting point for recursion, the ratios of successive order parameters shown in Table II are obtained. The ratios decrease toward the C-terminus, indicating increasing mobility. The ratio of order parameters fails to reach the value predicted for free rotation, indicating that the barriers to rotation are significant. It is also clear that the degree of restriction of rotation about the rotation axes increases away from the C-terminus. This is presumably due to the increased volume that must be rotated and increasing excluded volume effects [see Wittebort and Szabo (1978)]. These observations provide an internal reference for the degree of motional freedom available to an unstructured polypeptide chain. The cessation of large amplitude motion on the main chain at Arg 72 is precisely the point at which, according to both the crystal and solution structures of the protein, the main chain becomes tightly packed. This behavior suggests that tight molecular packing in the globular domain of the protein provides the dominant restriction to main-chain motion on the subnanosecond time scale and that the influence of local hydrogen bonding on the amplitude of main-chain dynamics is somewhat obscured. This is in contrast to the more vivid suppression of the amplitude of main-chain motion due to hydrogen bonding seen, for example, in the small, cyclic peptide cyclosporin A (Dellwo & Wand, 1989).

Acknowledgments

We thank Drs. D. Ecker, M. Rosenberg, and A. Shatzman for providing the expression vector for ubiquitin.

Supplementary Material Available

One table listing experimental and calculated T_1 and NOE values using the S^2 and τ_e obtained with $\Delta\delta$ equal to 160 ppm (3 pages). Ordering information is given on any current masthead page.

Registry No. Ubiquitin, 60267-61-0.

References

Bax, A., & Davis, D. G. (1985) *J. Magn. Reson. 65*, 355–360.
Bax, A., Griffey, R. H., & Hawkins, B. L. (1983) *J. Am. Chem. Soc. 105*, 7188–7190.
Boyd, J., Hommel, U., & Campbell, I. D. (1990) *Chem. Phys. Lett. 175*, 477–482.
Careri, G., Fasella, P., & Gratton, E. (1975) *CRC Crit. Rev. Biochem. 3*, 141–164.
Clore, G. M., Driscoll, P. C., Wingfield, P. T., & Gronenborn, A. M. (1990a) *Biochemistry 29*, 7387–7401.
Clore, G. M., Szabo, A., Bax, A., Kay, L. E., Driscoll, P. C., & Gronenborn, A. M. (1990b) *J. Am. Chem. Soc. 112*, 4989–4991.
Debrunner, P. G., & Fraunfelder, H. (1982) *Annu. Rev. Phys. Chem. 33*, 283–299.
Dellwo, M. J., & Wand, A. J. (1989) *J. Am. Chem. Soc. 111*, 4571–4578.
Dellwo, M. J., & Wand, A. J. (1991) *J. Magn. Reson. 91*, 505–516.
Di Stefano, D. L., & Wand, A. J. (1987) *Biochemistry 26*, 7272–7281.
Ecker, D. J., Butt, T. R., Marsh, J., Sternberg, E. J., Margolis, N., Monia, B. P., Jonnalagadda, S., Khan, M. I., Weber, P. L., Mueller, L., & Crooke, S. T. (1987) *J. Biol. Chem. 262*, 14213–14221.
Englander, S. W., & Kallenbach, N. R. (1984) *Q. Rev. Biophys. 16*, 521–655.
Goldman, M. (1984) *J. Magn. Reson. 60*, 437–452.
Gronenborn, A. M., Bax, A., Wingfield, P. T., & Clore, G. M. (1989) *FEBS Lett. 243*, 93–98.
Hartzell, C. J., Whitfield, M., Oas, T. G., & Drobny, G. P. (1987) *J. Am. Chem. Soc. 109*, 5966–5969.
Henry, E. R., & Szabo, A. (1985) *J. Chem. Phys. 82*, 4753–4761.
Hershko, A. (1988) in *Ubiquitin* (Rechsteiner, M., Ed.) pp 325–332, Plenum Press, New York.
Hiyama, Y., Niu, C., Silverton, J. V., Bavoso, A., & Torchia, D. A. (1988) *J. Am. Chem. Soc. 110*, 2378–2383.
Karplus, M., & McCammon, J. A. (1981) *CRC Crit. Rev. Biochem. 9*, 293–349.
Kay, L. E., Torchia, D. A., & Bax, A. (1989a) *Biochemistry 28*, 8972–8979.
Kay, L. E., Marion, D., & Bax, A. (1989b) *J. Magn. Reson. 84*, 72–84.
Kay, L. E., Clore, G. M., Bax, A., & Gronenborn, A. M. (1990) *Science 249*, 411–414.
Kay, L. E., Ikura, M., Zhu, G., & Bax, A. (1991) *J. Magn. Reson. 91*, 422–428.
Lipari, G., & Szabo, A. (1981a) *Biophys. J. 30*, 489–506.
Lipari, G., & Szabo, A. (1981b) *J. Chem. Phys. 75*, 2971–2976.
Lipari, G., & Szabo, A. (1982a) *J. Am. Chem. Soc. 104*, 4546–4559.
Lipari, G., & Szabo, A. (1982b) *J. Am. Chem. Soc. 104*, 4559–4570.
Marion, D., & Wüthrich, K. (1983) *Biochem. Biophys. Res. Commun. 113*, 967–974.
Molday, R. S., Englander, S. W., & Kallen, R. G. (1972) *Biochemistry 11*, 150–158.
Mueller, L. (1979) *J. Am. Chem. Soc. 101*, 4481–4484.
Nirmala, N. R., & Wagner, G. (1988) *J. Am. Chem. Soc. 110*, 7557–7559.
Nirmala, N. R., & Wagner, G. (1989) *J. Magn. Reson. 82*, 659–661.
Rance, M., Sorensen, O. W., Bodenhausen, G., Wagner, G., Ernst, R. R., & Wüthrich, K. (1983) *Biochem. Biophys. Res. Commun. 117*, 479–485.
Shaka, A. J., Keller, J., & Freeman, R. (1983) *J. Magn. Reson. 53*, 313–340.
Sklenar, V., Torchia, D., & Bax, A. (1987) *J. Magn. Reson. 73*, 375–379.
Solomon, I. (1955) *Phys. Rev. 99*, 559–565.
Taylor, R., & Kennard, O. (1983) *Acta Crystallogr. B39*, 133–138.
Vijay-Kumar, S., Bugg, C. E., & Cook, W. J. (1987) *J. Mol. Biol. 194*, 531–544.
Wallach, D. (1967) *J. Am. Chem. Soc. 47*, 5258–5268.
Weber, P. L., Brown, S. C., & Mueller, L. (1987) *Biochemistry 26*, 7282–7290.
Williams, R. J. P. (1989) *Eur. J. Biochem. 183*, 479–497.
Wittebort, R. J., & Szabo, A. (1978) *J. Chem. Phys. 69*, 1722–1736.